

## Supporting Information

### Enhancement of the Anti-Aggregation Activity of a Molecular Chaperone Using a Rationally Designed Post-Translational Modification

Philip R. Lindstedt,<sup>†</sup> Francesco A. Aprile,<sup>†</sup> Maria J. Matos,<sup>†</sup> Michele Perni,<sup>†</sup> Jean B. Bertoldo,<sup>†</sup> Barbara Bernardim,<sup>†</sup> Quentin Peter,<sup>†</sup> Gonzalo Jiménez-Osés,<sup>‡,§</sup> Tuomas P. J. Knowles,<sup>†</sup> Christopher M. Dobson,<sup>†</sup> Francisco Corzana,<sup>‡</sup> Michele Vendruscolo,<sup>\*,†</sup> and Gonçalo J. L. Bernardes<sup>\*,†,§</sup>

<sup>†</sup>Department of Chemistry, University of Cambridge, Lensfield Road, Cambridge CB2 1EW (UK)

<sup>‡</sup>Departamento de Química, Universidad de La Rioja, Centro de Investigación en Síntesis Química, 26006 Logroño (Spain)

<sup>§</sup>CIC bioGUNE, Bizkaia Technology Park, Building 801A, 48170 Derio (Spain)

<sup>§</sup>Instituto de Medicina Molecular, Faculdade de Medicina, Universidade de Lisboa, Avenida Professor Egas Moniz, 1649-028, Lisboa (Portugal)

Correspondence should be addressed to G.J.L.B. or M.V.:  
E-mail: [gb453@cam.ac.uk](mailto:gb453@cam.ac.uk) or [mv245@cam.ac.uk](mailto:mv245@cam.ac.uk)

## Table of Contents

<b>Materials and Methods</b>	3
Hsp70 expression and purification	3
LC-MS method for analysis of protein conjugation	3
Protein conjugation	4
Enzymatic digestion and LC-MS/MS analysis	5
Molecular dynamics (MD) simulations on Hsp-caaNBF	5
Colorimetric ATPase assay	6
Luciferase refolding assays	7
Circular dichroism	7
$\alpha$ -Synuclein aggregation assay	8
<i>C. elegans</i> growth	8
Chaperone transduction into <i>C. elegans</i>	9
<i>C. elegans</i> motility experiments	9
<i>C. elegans</i> imaging	9
SDS-page method for analysis of protein conjugation	10
Synthesis of fluorescent caaNBF and NBF control	10
<b>Supporting Figures</b>	13
<b>Figure S1.</b> Variations of the estimated Hsp70 cysteine pKa values during a 650 ns MD trajectory.	13
<b>Figure S2.</b> LC-MS of HSP70.	13
<b>Figure S3.</b> LC-MS of Hsp70-caa.	14
<b>Figure S4.</b> MS/MS sequence coverage.	14
<b>Figure S5.</b> Molecular dynamics (MD) simulations in explicit water.	15
<b>Figure S6.</b> $\alpha$ -synuclein ATPase contamination control.	15
<b>Figure S7.</b> Control $\alpha$ -synuclein aggregation assays.	16
<b>Figure S8.</b> Comparison of the histograms of combined <i>C. elegans</i> treatment populations and scatter matrices.	16
<b>Figure S9.</b> Characterizing unspecific benefits of Hsp-caaNBF treatment on wild-type worms.	17
<b>Figure S10.</b> $^1\text{H}$ and $^{13}\text{C}$ NMR of caaNBF.	18
<b>Figure S11.</b> $^1\text{H}$ and $^{13}\text{C}$ NMR of NBF control.	19
<b>References</b>	20

## Materials and Methods

### Hsp70 expression and purification

Recombinant human Hsp70 (*human Hsp70 1A*, GenBank ID: [NP005336](#)) with an *N*-terminal hexa-histidine tag was overexpressed in *E. coli* BL21 (DE3) Gold Strain from a pET-28b vector (Merk KGaA, Darmstadt, Germany). Hsp70 was purified through Ni-NTA affinity chromatography as described previously.<sup>1</sup> Monomeric protein was then further isolated by size exclusion chromatography (SEC) using a Superdex 26/60 G75 column (GE Healthcare LifeSciences, Little Chalfont, U.K.). Concentration measurements were determined by measuring the absorbance of the solution at 280 nm and using the theoretical extinction coefficient calculated with ExPASy ProtParam. Protein was then aliquoted, and flash frozen in liquid nitrogen prior to long-term storage at -80 °C.

### LC-MS method for analysis of protein conjugation

LC-MS was performed on a Xevo G2-S TOF mass spectrometer coupled to an Acquity UPLC system using an Acquity Q6 UPLC BEH300 C4 column (1.7 mm, 2.1 × 50 mm). Solvents A, water with 0.1% formic acid and B, 71% acetonitrile, 29% water and 0.075% formic acid were used as the mobile phase at a flow rate of 0.2 mL min<sup>-1</sup>. The gradient was programmed as follows: 72% A to 100% B after 25 min then 100% B for 2 min and after that 72% A for 18 min. The electrospray source was operated with a capillary voltage of 2.0 kV and a cone voltage of 40 V. Nitrogen was used as the desolvation gas at a total flow of 850 L h<sup>-1</sup>. Total mass spectra were reconstructed from the ion series using the MaxEnt algorithm preinstalled on MassLynx software (v. 4.1 from Waters) according to the manufacturer's instructions. To obtain the ion series described, the major peak(s) of the chromatogram were selected for integration and further analysis.

## Protein conjugation

Reaction of Hsp70 with caa: To an Eppendorf with 28.54  $\mu\text{L}$  of TrisHCl 20 mM, at pH 8.0, and 3.19  $\mu\text{L}$  of DMF, was added a 7.46  $\mu\text{L}$  aliquot of a stock solution of Hsp70 (53.6  $\mu\text{M}$ ) and the resulting mixture was vortexed for 10 s. Afterwards, a 0.5291 mM solution of caa (0.81  $\mu\text{L}$ , 1 equiv.) in DMF was added and the reaction shook for 1 h, at 37  $^{\circ}\text{C}$ . A 10  $\mu\text{L}$  aliquot was analysed by LC-MS and full conversion to the expected product was observed (calculated mass, 72285; observed mass, 72282).

Reaction of Hsp70 with caaNBF: To an Eppendorf with 28.54  $\mu\text{L}$  of TrisHCl 20 mM, at pH 8.0, and 3.05  $\mu\text{L}$  of DMF, was added a 7.46  $\mu\text{L}$  aliquot of a stock solution of Hsp70 (53.6  $\mu\text{M}$ ) and the resulting mixture was vortexed for 10 s. Afterwards, a 0.4195 mM solution of caaNBF (0.95  $\mu\text{L}$ , 1 equiv.) in DMF was added and the reaction shook for 1 h, at 37  $^{\circ}\text{C}$ . A 10  $\mu\text{L}$  aliquot was analysed by LC-MS and full conversion to the fluorescent expected product was observed by SDS-PAGE (calculated mass, 72463).

### **Enzymatic digestion and LC-MS/MS analysis**

All LC-MS/MS experiments were performed using a nanoAcquity UPLC (Waters Corp., Milford, MA) system and an LTQ Orbitrap Velos hybrid ion trap mass spectrometer (Thermo Scientific, Waltham, MA). Separation of peptides was performed by reverse-phase chromatography using a Waters reverse phase nano column (HSS T3 C18, 75  $\mu\text{m}$  i.d. x 250 mm, 1.7  $\mu\text{m}$  particle size) at flow rate of 300 nL/min. Peptides were initially loaded onto a pre-column (Waters UPLC Trap Symmetry C18, 180  $\mu\text{m}$  i.d. x 20 mm, 5  $\mu\text{m}$  particle size) from the nanoAcquity sample manager with 0.1% formic acid for 3 min at a flow rate of 5  $\mu\text{L}/\text{min}$ . After this period, the column valve was switched to allow the elution of peptides from the pre-column onto the analytical column. Solvent A was water + 0.1% formic acid and solvent B was acetonitrile + 0.1% formic acid. The linear gradient employed was 5-40% B in 40 min. The LC eluent was sprayed into the mass spectrometer by means of a nanospray ion source. All  $m/z$  values of eluting ions were measured in the Orbitrap Velos mass analyzer, set at a resolution of 30000. Data dependent scans (Top 20) were employed to automatically isolate and generate fragment ions by collision-induced dissociation in the linear ion trap, resulting in the generation of MS/MS spectra. Ions with charge states of  $2^+$  and above were selected for fragmentation. Post-run, the data was processed using Protein Discoverer (version 1.4., ThermoFisher). Briefly, all MS/MS data were converted to mgf files and these were submitted to the Mascot search algorithm (Matrix Science, London, UK) and searched against custom databases containing the HSP70 protein sequences along with common contaminant sequences, such as keratins, trypsin etc., (<http://www.thegpm.org/crap/>) and applying variable modifications of oxidation (M), deamidation (NQ), and custom modifications of caaNBF (C), and using peptide tolerances of 25 ppm (MS) and 0.8 Da (MS/MS). Peptide identifications were accepted if they could be established at greater than 95.0% probability. Significant hits that suggested that the expected Cys modifications were bound to peptides were then verified by manual inspection of the MS/MS data.

### **Molecular dynamics (MD) simulations on Hsp-caaNBF.**

A homology model of Hsp70 obtained through SWISS-MODEL<sup>2</sup> was used as starting coordinates for the protein in the simulations. MD simulations were carried out with AMBER 18 package,<sup>3</sup> implemented with ff14SB,<sup>4</sup> and GAFF<sup>5</sup> force fields. Parameters for the unnatural residue (caaNBF) were generated with the antechamber module of AMBER, using GAFF force field and with partial charges set to fit the electrostatic potential generated with HF/6-31G(d) by RESP.<sup>6</sup> The charges were calculated according to the Merz-Singh-Kollman scheme using

Gaussian 16.<sup>7</sup> Hsp70 protein or the corresponding conjugates were immersed in a water box with a 10 Å buffer of TIP3P water molecules<sup>8</sup> and neutralized by adding explicit counter ions. A two-stage geometry optimization approach was performed. The first stage minimizes only the positions of solvent molecules and ions, and the second stage is an unrestrained minimization of all the atoms in the simulation cell. The systems were then heated by incrementing the temperature from 0 to 300 K under a constant pressure of 1 atm and periodic boundary conditions. Harmonic restraints of 10 kcal·mol<sup>-1</sup> were applied to the solute, and the Andersen temperature coupling scheme<sup>9</sup> was used to control and equalize the temperature. The time step was kept at 1 fs during the heating stages, allowing potential inhomogeneities to self-adjust. Hydrogen atoms were kept fixed through the simulations using the SHAKE algorithm.<sup>10</sup> Long-range electrostatic effects were modelled using the particle-mesh-Ewald method.<sup>11</sup> An 8 Å cutoff was applied to Lennard-Jones interactions. Each system was equilibrated for 2 ns with a 2-fs time step at a constant volume and temperature of 300 K. Production trajectories were then run for additional 0.65 μs (native Hsp70) or 0.5 μs (for the conjugates) under the same simulation conditions. PROPKA algorithm (PARSE force-field) on Hsp70 structures derived from the MD simulation was used to perform a theoretical calculation of the pKa values of the different cysteine residues of the protein.<sup>12</sup>

### **Colorimetric ATPase assay**

The ATPase assay was performed as described before.<sup>13</sup> Briefly, the ATPase reagent was made by combining 0.081% W/V Malachite Green with 2.3% W/V poly-vinyl alcohol, 5.7% W/V ammonium heptamolybdate in 6M HCl, and water in 2:1:1:2 ratios (all purchased from Sigma with no further purification). ATPase activity was tested by incubating 2 μM of the chaperone with 1mM ATP, with and without the presence of 70 μM α-synuclein monomer, in assay buffer (0.017% Triton X-100, 100 mM Tris-HCl, 20 mM KCl, and 6 mM MgCl<sub>2</sub>, pH 7.4) at 37 °C for 3 h. At the end of incubation 25 μL of the reaction was added to a well in a 96 well plate, followed by 80 μL of the ATPase reagent and 10 μL of 34% sodium citrate to halt any further ATP hydrolysis, the mixture was allowed to incubate for 15 min at 37 °C before absorbance at 620 nm was measured using a CLARIOstar plate reader (BMG Labtech, Allmendgruen, Germany), a control sample of ATP alone in buffer treated exactly the same and subtracted from the sample absorbance's to account for intrinsic ATP hydrolysis. To account for variability in measurements a phosphate standard curve was created for each day of measurements.

### **Luciferase refolding assays**

The refolding of chemically denatured firefly luciferase (Promega Corp., Madison WI) by labelled or unlabeled Hsp70 was conducted as described previously (36). Luciferase was diluted 42-fold into denaturing buffer (50 mM Tris pH 7.4, 150 mM KCl, 5 mM MgCl<sub>2</sub>, 5 mM dithiothreitol, 6 M guanidinium hydrochloride), and the denaturing reaction was allowed to proceed for 40 min at 25 °C. Then, a 1 µL aliquot was taken and placed into 125 µL of refolding buffer (50mM Tris pH 7.4, 150 mM KCl, 5 mM MgCl<sub>2</sub>, 1 mM ATP) supplemented with 1 µM of labelled or unlabeled Hsp70 and 0.5 µM of DNAJB1 (Cambridge Biosciences Ltd., Cambridge, U.K.) incubated at 25 °C. Finally, 2.5 µL aliquots of the refolding reaction were then taken and added to 47.5 µL of luciferase assay reagent (Promega Corp., Madison WI) at various timepoints, activity was then measured with a CLARIOstar plate reader (BMG Labtech, Allmendgruen, Germany). Heat denatured refolding of luciferase was performed as previously described (36). Briefly, Hsp70's (4 µM) were incubated in refolding buffer supplemented with 1 mM ATP for 15 min at room temperature. Next, luciferase (80 nM) was added and incubated for a further 10 min. Then DNAJB1 (Cambridge Biosciences Ltd., Cambridge, U.K.) (1 µM) was added and the mixture was heat shocked at 42 °C for 10 min. The reactions were then immediately removed to room temperature and luciferase activity was checked at various timepoints by diluting 2.5 µL samples of the refolding reactions into 47.5 µL of luciferase reagent (Promega Corp., Madison WI), activity was then measured with a CLARIOstar plate reader (BMG Labtech, Allmendgruen, Germany).

### **Circular dichroism**

Circular dichroism (CD) spectroscopy was used to analyze protein secondary structure in solution. Samples were concentrated to 10 µM in NaP<sub>i</sub> buffer (50 mM, pH 8.0). CD measurements were recorded using a Chirascan spectrophotometer equipped with a Quantum TC125 temperature control unit (25 °C). The data was acquired in a 0.1 cm path length with a response time of 1 s, a per-point acquisition delay of 5 ms and a pre- and post-scan delay of 50 ms. Spectra were averaged over three scans, in a wavelength range from 190 nm to 260 nm, and the spectrum from a blank sample containing only buffer was subtracted from the averaged data. The structural stability was analyzed by monitoring the CD signal at 207 nm from 20 ° to 85 °C at a rate of 0.5 °C min<sup>-1</sup>. Data points were acquired every 0.1 °C with a bandwidth of 1 nm.

### **$\alpha$ -Synuclein aggregation assay**

Seeded anti-aggregation assays were ran as described previously.<sup>1</sup> Briefly, 70  $\mu$ M  $\alpha$ -synuclein monomer in 50 mM Tris (pH 7.4), 150 mM KCl, 5 mM MgCl<sub>2</sub>, 20  $\mu$ M THT, 5% preformed fibrils, and 5 mM ATP at 37 °C supplemented with 1  $\mu$ M of the appropriate chaperone or small molecule. Plates were sealed to avoid evaporation and the reaction was monitored by measuring the emission at 480 nm after excitation at 440 nm using a CLARIOstar plate reader (BMG Labtech, Allmendgruen, Germany). Data was normalized by fitting a Boltzmann sigmoidal function to the respective controls for each condition in Prism and using the calculated plateau value as the maximum. First generation fibrils were created by incubating 300  $\mu$ L of 70  $\mu$ M monomeric  $\alpha$ -synuclein (50 mM Tris pH 7.4, 150 mM KCl, 5 mM MgCl<sub>2</sub>, 0.01% NaN<sub>3</sub>) at 37C for 4 days shaking at 200 rpm. The resulting fibrils were centrifuged as 16000 g, the pellet was washed twice with 300  $\mu$ L of buffer and then sonicated for 1 min at 10% maximum power with 30% cycles using a probe sonicator (Bandelin, Sonoplus HD 2070). Second generation fibrils were then created by incubating 100  $\mu$ M monomeric  $\alpha$ -synuclein with 10  $\mu$ M of the first-generation fibrils (in terms of original monomer concentration) in 500  $\mu$ L of buffer for 13–14 h under quiescent conditions. Finally, the second-generation fibrils were sonicated for 20 s, 10% power, 30% cycles to generate the seeds for the assay. To quantify the monomer after the aggregations the reactions were extended for 48 h to maximally deplete the monomer in each condition. The samples were then pooled together and spun down on an ultracentrifuge at 80000 RPM for 1hr (TLA100 rotor, Optima™ TLX Ultracentrifuge, Beckmann Coulter, Indianapolis, IN). 1  $\mu$ L of sample was then mixed with 2  $\mu$ L of NuPAGE LDS Sample Buffer and 5  $\mu$ L of PBS, after heating for 10 mins at 95 °C the samples were ran on a NuPAGE Bis-Tris mini gel (10x 10 cm) with 4-12% gradient polyacrylamide concentration. The gel was then stained using InstantBlue™ (Sigma Aldrich).

### ***C. elegans* growth**

Worms were propagated and using established methods.<sup>14</sup> Briefly, worms were synchronized for experiments by treatment with hypochlorite and then hatching overnight in M9 buffer (3 g/L KH<sub>2</sub>PO<sub>4</sub>, 6 g/L Na<sub>2</sub>HPO<sub>4</sub>, 5 g/L NaCl, 7.5 g/L casein). The hatched worms were then cultured at 20 C on nematode growth medium (NGM) (1 mM CaCl<sub>2</sub>, 1 mM MgSO<sub>4</sub>, 5  $\mu$ g/mL cholesterol, 250 mM KH<sub>2</sub>PO<sub>4</sub> (pH 6), 17 g/L agar, 3 g/L NaCl, 7.5 g/L casein) plates which were seeded with OP50 *E. coli*. Cultures of OP50 were grown to saturation by inoculating 50 mL of LB medium (10 g/L tryptone, 10 g/L NaCl, 5 g/L yeast extract) with OP50 and



incubating the culture at 37 °C for 16 h. Plates were seeded with OP50 by placing 350 µL of the saturated culture on each plate and leaving it for 2–3 days at 20 °C. After day 3 of synchronization worms were moved and placed onto NGM plates containing 75 µM 5-fluoro-2'-deoxy-uridine (FUDR) to inhibit the viability of eggs laid by the adults.

### **Chaperone transduction into *C. elegans***

To prepare the chaperones for transduction a reagent traditionally used for lipid mediated transfection of cells was adapted.<sup>15</sup> Firstly, 20 µL of 20 µM chaperone was incubated for 30 min with 40 µL of PULSin reagent (PolyPlus-transfection SA) in a final volume of 1 mL supplemented with the provided PULSin buffer. Then, between 100–200 worms were added to the mixture for each condition and replica in a 1.5 mL Eppendorf tube and incubated for 5 h then re-plated on solid media overnight to be screened the following morning.

### ***C. elegans* motility experiments**

To screen the worms for changes in motility the same procedure used in,<sup>16, 17</sup> the full 1 mL of the worm/transduction mixture was added to 9 cm NGM plates that were unseeded with OP50 the morning after incubation, which contained 6 mL of M9 buffer, bringing the total screening volume to 7 mL. Immediately after the worms were transferred from their Eppendorf's to the screening plates, they were placed onto an imaging platform and 30 FPS movies were taken for 1 min to record the swimming of the worms. The videos were then analysed using custom made tracking software and further statistical calculations were performed with SciPy.

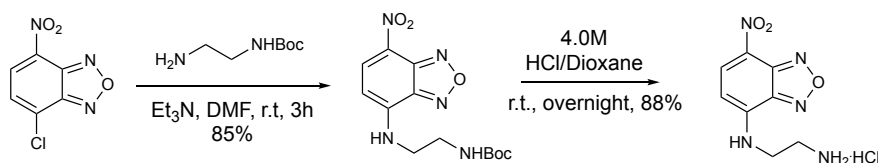
### ***C. elegans* imaging**

To visualize the inclusions in the worms, 4 days after the transduction worms were mounted onto 5% agarose pads on glass microscope slides and anesthetized with 40 mM NaN<sub>3</sub>, then compressed by placing a glass coverslip on top of the suspended worms. Images were taken with a Zeiss Axio Observer D1 fluorescence microscope (Carl Zeiss Microscopy GmbH) with a 20x objective and 49002 ET-EGFP-FITC-Cy2 filter (Chroma Technology Corp.). Analysis of the images was done in ImageJ software (National Institutes of Health) and a custom python-based program.

### SDS-page method for analysis of protein conjugation

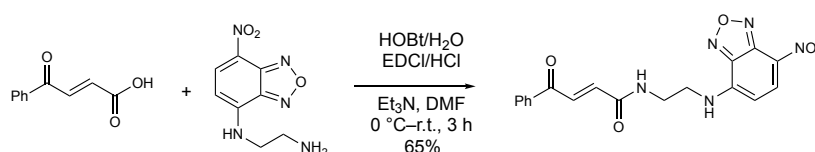
The incubation solution (5.0  $\mu$ L) was transferred to tube and NuPAGE LDS Sample Buffer (4x, 2.5 mL), NuPAGE Reducing Agent (10x, 1 mL), and H<sub>2</sub>O (1.5 mL) were added to the tube. The solution was heated at 70 °C for 10 min. The heated solution was loaded to NuPAGE Bis-Tris mini gel (10 x 10 cm) with 4-12% gradient polyacrylamide concentration, and then the conjugation reaction was analysed by electrophoresis (200 V). The buffering system employed was 1x SDS Running Buffer (NuPAGE MES SDS Running Buffer, 20x, pH 7.3, 50 to 950 mL deionized water). For reduced samples, 500 mL of NuPAGE. Antioxidant was added to each 200 mL 1x SDS running buffer. After 35 min, the intensities of fluorescence were analysed. Then, the gel was stained with 0.5% of Ruby. The gel was mixed overnight at room temperature and read the day after. After wash the gel, coomassie (0.5%) was added and the gel was read 2 h after mixing at room temperature.

### Synthesis of fluorescent caaNBF and NBF control



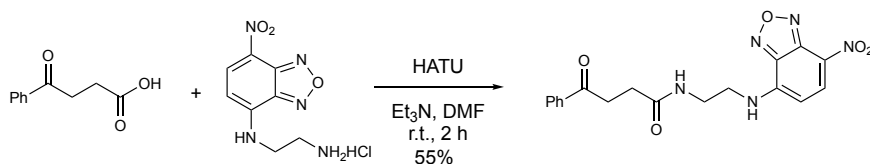
*tert*-butyl (2-((7-nitrobenzo[*c*][1,2,5]oxadiazol-4-yl)amino)ethyl)carbamate was prepared following a reported procedure.<sup>18</sup> Under an argon atmosphere, 4-chloro-7-nitrobenzofurazan-NBD-Cl (398 mg, 2.0 mmol, 1 equiv.) was dissolved in anhydrous DMF (10 mL). After adding triethylamine (276  $\mu$ L, 2.0 mmol, 1 equiv.) and *N*-Boc-1,2-diaminoethane (348  $\mu$ L, 2.4 mmol, 1.2 equiv.), the mixture was stirred at room temperature for 3 h. After completion of the reaction followed by TLC (1:1, EtOAc/hexanes, using UV and KMnO<sub>4</sub> staining solution), the reaction mixture was poured into a saturated aqueous ammonium chloride solution (30 mL). The mixture was extracted with ethyl acetate (3 x 40 mL), and the organic layer was washed with water (50 mL) and brine (50 mL) and then dried over MgSO<sub>4</sub>. After solvent removal under reduced pressure, brown oily *N*-Boc protected intermediate (550 mg, 1.7 mmol, 85%) was obtained with spectral data in accordance with the ones reported in the literature.<sup>18</sup> <sup>1</sup>H NMR (400 MHz, Chloroform-*d*)  $\delta$  8.48 (d, *J* = 8.7 Hz, 1H), 8.01 (br s, 1H), 6.16 (d, *J* = 8.6 Hz, 1H), 5.09 (br s, 1H), 3.59 (br s, 4H), 1.46 (s, 9H); HRMS ESI<sup>+</sup> (*m/z*): Calcd. For C<sub>13</sub>H<sub>18</sub>N<sub>5</sub>O<sub>5</sub><sup>+</sup> [M + H]<sup>+</sup> 324.1302, found 324.1302.

***N*<sup>1</sup>-(7-nitrobenzo[*c*][1,2,5]oxadiazol-4-yl)ethane-1,2-diamine** Under an argon atmosphere, the Boc-protected intermediate (524 mg, 1.62 mmol, 1 equiv.) was dissolved in a 4.0 M solution of HCl in dioxane (12 mL). The solution was shaded from the light and stirred overnight. After confirming completion of the reaction by TLC (9:1, CH<sub>2</sub>Cl<sub>2</sub>/MeOH, using UV and KMnO<sub>4</sub> staining solution), the reaction solution was evaporated under reduced pressure and the brown solid (370.0 mg, 1.42 mmol, 88%) used in the next step. The spectral data in accordance with the one reported in the literature.<sup>18</sup> <sup>1</sup>H NMR (400 MHz, Methanol-*d*<sub>4</sub>) δ 8.54 (d, *J* = 8.7 Hz, 1H), 6.47 (d, *J* = 8.7 Hz, 1H), 3.89 (t, *J* = 6.2 Hz, 2H), 3.34 (t, *J* = 6.3 Hz, 2H); HRMS ESI<sup>+</sup> (*m/z*): Calcd. C<sub>8</sub>H<sub>10</sub>N<sub>5</sub>O<sub>3</sub><sup>+</sup> [M + H]<sup>+</sup> 224.0778, found 224.0784.



**(*E*)-*N*-(2-((7-nitrobenzo[*c*][1,2,5]oxadiazol-4-yl)amino)ethyl)-4-oxo-4-phenylbut-2-enamide** Under an argon atmosphere, 3-benzoylacrylic acid (108.0 mg, 0.61 mmol, 1 equiv.) was dissolved in anhydrous DMF and triethylamine (170 μL, 1.22 mmol, 2.0 equiv.) was added dropwise. To the solution were sequentially added 1-hydroxybenzotriazole hydrate (111.5 mg, 0.73 mmol, 1.2 equiv.), *N*-(3-Dimethylaminopropyl)-*N*'-ethylcarbodiimide hydrochloride (140.0 mg, 0.73 mmol, 1.2 equiv.) and *N*<sup>1</sup>-(7-nitrobenzo[*c*][1,2,5]oxadiazol-4-yl)ethane-1,2-diamine (149.5 mg, 0.61 mmol, 1 equiv.) under ice-cooling. Then, the reaction was shaded from light, and after reaching room temperature, stirred for 3 h. After detecting full conversion of the reactants by TLC (95:5, CH<sub>2</sub>Cl<sub>2</sub>/MeOH, using UV and KMnO<sub>4</sub> staining solution), the reaction was poured into an aqueous HCl solution (0.5 M, 40 mL) and extracted with CH<sub>2</sub>Cl<sub>2</sub> (3 x 40 mL). The combined organic phase was washed with saturated Na<sub>2</sub>CO<sub>3</sub> (2 x 40 mL) and brine (2 x 40 mL), then dried over MgSO<sub>4</sub>. Removal of all volatiles *in vacuo* gave the compound as a yellow/brown solid (151.0 mg, 0.40 mmol, 65%). The product was obtained in good purity (<sup>1</sup>H NMR analysis), the remainder of the material being composed of a mixture of unidentified minor components. Attempts to purify the compound by chromatography (silica, triethylamine washed silica, alumina, florisil) or recrystallization led to further decomposition. The material at ca. 95% purity was sufficient for subsequent experiments: R<sub>f</sub> = 0.71 (95:5, CH<sub>2</sub>Cl<sub>2</sub>/MeOH); <sup>1</sup>H NMR (500 MHz, DMSO-*d*<sub>6</sub>) δ 8.80 (t, *J* = 5.8 Hz, 1H), 8.52 (d, *J* = 8.8 Hz, 1H), 7.98 (d, *J* = 6.9 Hz, 2H), 7.74 (d, *J* = 15.3 Hz, 1H), 7.69 (t, *J* = 7.4 Hz, 1H), 7.56 (t, *J*

= 7.8 Hz, 2H), 6.91 (d,  $J = 15.3$  Hz, 1H), 6.47 (d,  $J = 9.0$  Hz, 1H), 3.63 (bs, 2H), 3.56 – 3.47 (m, 2H);  $^{13}\text{C}$  NMR (125 MHz,  $\text{DMSO-}d_6$ )  $\delta$  189.8, 164.1, 145.4, 144.6, 137.9, 136.5, 136.1, 133.8, 132.1, 129.0, 128.6, 128.2, 99.3, 45.7, 29.0; HRMS ESI<sup>+</sup> ( $m/z$ ): Calcd.  $\text{C}_{18}\text{H}_{16}\text{N}_5\text{O}_5^+$  [ $\text{M} + \text{H}$ ]<sup>+</sup> 382,1146, found 382.1133.



**N-(2-((7-nitrobenzo[c][1,2,5]oxadiazol-4-yl)amino)ethyl)-4-oxo-4-phenylbutanamide**

In a round-bottom flask, 4-oxo-4-phenylbutanoic acid (48.3 mg, 0.29 mmol, 1 equiv.) was dissolved in 4 mL of anhydrous DMF and triethylamine (86  $\mu\text{L}$ , 0.63 mmol, 2.2 equiv.) was added dropwise. To the solution was added HATU (112.0 mg, 0.30 mmol, 1.1 equiv.) Then, the reaction was shaded from light and stirred for 10 min. After this time, the amine *N*<sup>1</sup>-(7-nitrobenzo[c][1,2,5]oxadiazol-4-yl)ethane-1,2-diamine (77.0 mg, 0.3 equiv., 1.1 equiv.) was added as a solid and the reaction mixture stirred for an additional 2 at room temperature. After detecting full conversion of the reactants by TLC (10%,  $\text{CH}_2\text{Cl}_2/\text{MeOH}$ ), the reaction was diluted with AcOEt (30 mL) and washed with  $\text{H}_2\text{O}$  (2 x 20 mL), HCl 1.5 M solution (2 x 20 mL),  $\text{NaHCO}_3$  (2 x 20 mL) and brine (1 x 20 mL). The organic phase was then dried over  $\text{MgSO}_4$ . Removal of all volatiles *in vacuo* gave the control compound as a brown gummy solid. The resulting material was triturated in  $\text{CHCl}_3$  to provide the product as a brown solid (61.0 mg, 0.16 mmol, 55%).  $R_f = 0.75$  (95:5,  $\text{CH}_2\text{Cl}_2/\text{MeOH}$ );  $^1\text{H}$  NMR (400 MHz,  $\text{DMSO-}d_6$ )  $\delta$  9.40 (s, 1H), 8.53 (d,  $J = 8.9$  Hz, 1H), 8.15 (t,  $J = 5.9$  Hz, 1H), 7.92 (d,  $J = 7.2$  Hz, 2H), 7.63 (t,  $J = 7.4$  Hz, 1H), 7.51 (t,  $J = 7.6$  Hz, 2H), 6.43 (d,  $J = 9.0$  Hz, 1H), 3.55 (bs, 2H), 3.38 (m, 2H), 3.22 (t,  $J = 6.6$  Hz, 2H), 2.45 (t,  $J = 6.6$  Hz, 2H);  $^{13}\text{C}$  NMR (100 MHz,  $\text{DMSO-}d_6$ )  $\delta$  199.21, 172.43, 145.95, 144.93, 144.50, 138.43, 136.95, 133.57, 129.11, 128.23, 121.28, 99.63, 43.51, 37.95, 33.73, 29.66; FTIR (neat,  $\text{cm}^{-1}$ ): 3314, 1685, 1651, 1584, 1545, 1506, 1358, 1303, 1243, 1128, 1026, 903; HRMS ESI<sup>+</sup> ( $m/z$ ): Calcd.  $\text{C}_{18}\text{H}_{18}\text{N}_5\text{O}_5^+$  [ $\text{M} + \text{H}$ ]<sup>+</sup> 384,3715, found 384.3729.

## Supporting Figures

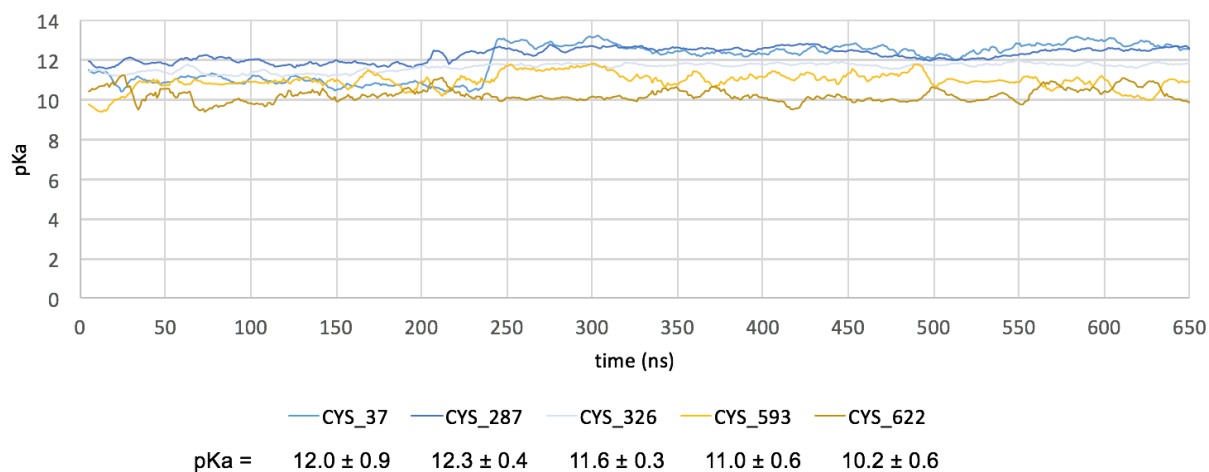


**Figure S1.** Variations of the estimated Hsp70 cysteine pKa values through a 650-ns MD trajectory. Evolution of pK<sub>a</sub> values calculated with PROPKA<sup>12</sup> along the 650 ns MD simulations started from a homology model of Hsp70 obtained using SWISS-MODEL.<sup>2</sup>

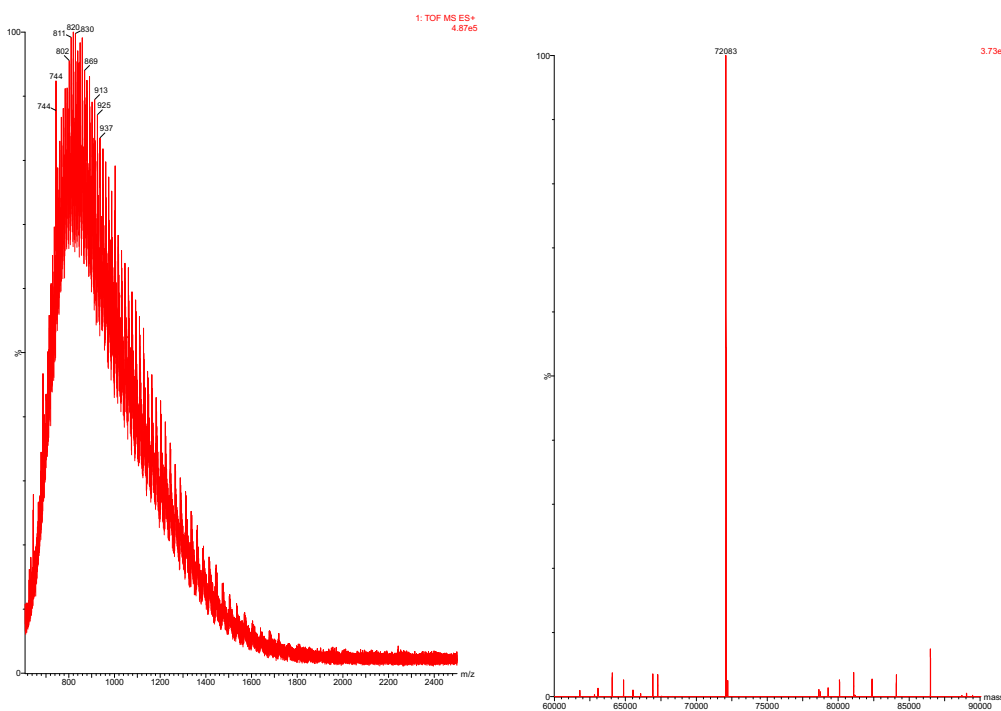


**Figure S2.** Combined ion series and deconvoluted spectra of HSP70.

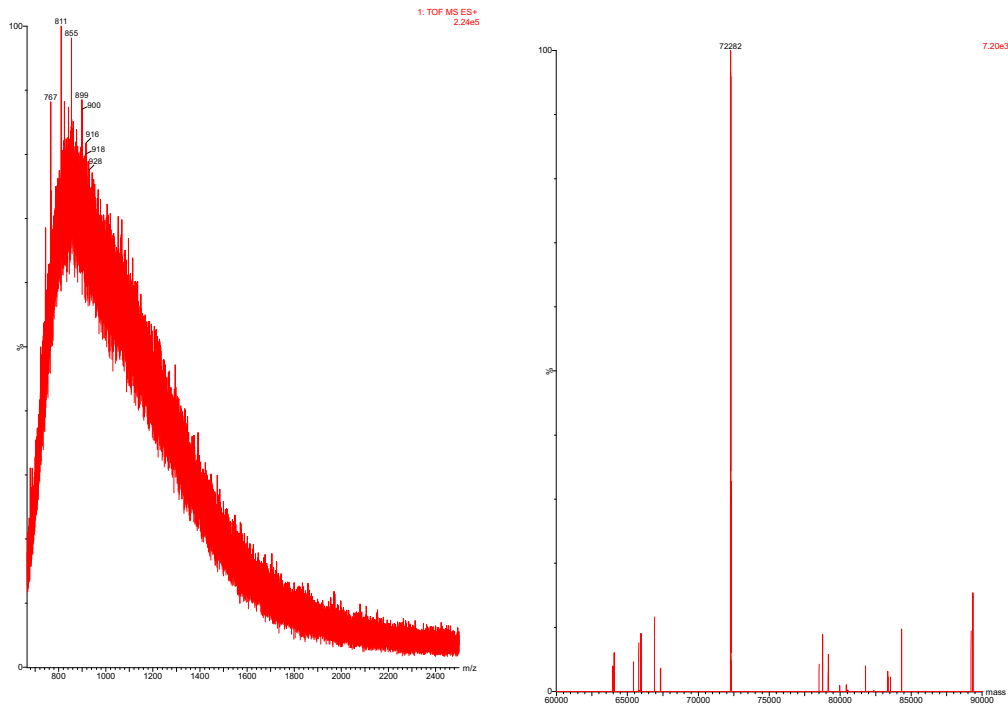


**Figure S3.** Combined ion series and deconvoluted spectra of the reaction of Hsp70 with caa.

**Protein sequence coverage: 92%**

Matched peptides shown in **bold red**.

```

1  MGSSHHHHHH  SGLVPRGSH  MAKAAAIGID  LGTTYSCVGV  FQHGKVEIIA
51  NDQGNRTTPS  YVAFTDTERL  IGDAAKNQVA  LNPQNTVPDA  KRLIGRKFGE
101  PVVQSDMKHW  PFQVINDGDK  PKVQVSYKGD  TKAFYPPEIS  SMVLTKMKEI
151  AEAYLGYPVT  NAVITVPAYF  NDSQRQATKD  AGVIAGLNVL  RIINEPTAAA
201  IAYGLDRTGK  GERNLIFDL  GGGTFDVSIL  TIDDGIFEVK  ATAGDTHLGG
251  EDFDNRLVNH  FVEEFKRKHK  KDISQNKRAV  RRLRTACERA  KRTLSSSTQA
301  SLEIDSLFEG  IDFYTSITRA  RFEELCSDLF  RSTLEPVEKA  LRDAKLDKAQ
351  IHDLVLVGGG  TRIPKVQKLL  QDFNNGRDLN  KSINPDEAVA  YGAAVQAAIL
401  MGDKSENVQD  LLLLDVAPLS  LGLETAGGVM  TALIKRNSTI  PTKQTQIFTT
451  YSDNQPGVLI  QVYEGERAMT  KNNLLGRFE  LSGIPPAPRG  VPQIEVTFDI
501  DANGILNVTA  TDKSTGKANK  ITITNDKGR  SKEEIERMVQ  EAEKYKAED
551  VQRERVSAKN  ALESYAFNMK  SAVEDEGLKG  KISEADKKKV  LDKCQEVISW
601  LDANTLAEKD  EFEHKRKELE  QVCNPIISGL  YQGAGGPGPG  GFQAQGPKGG
651  SGSGPTIEEV  D

```

**Figure S4.** Sequence coverage of Hsp70-caa after digestion and MS/MS analysis; detected sequences are shown in red.

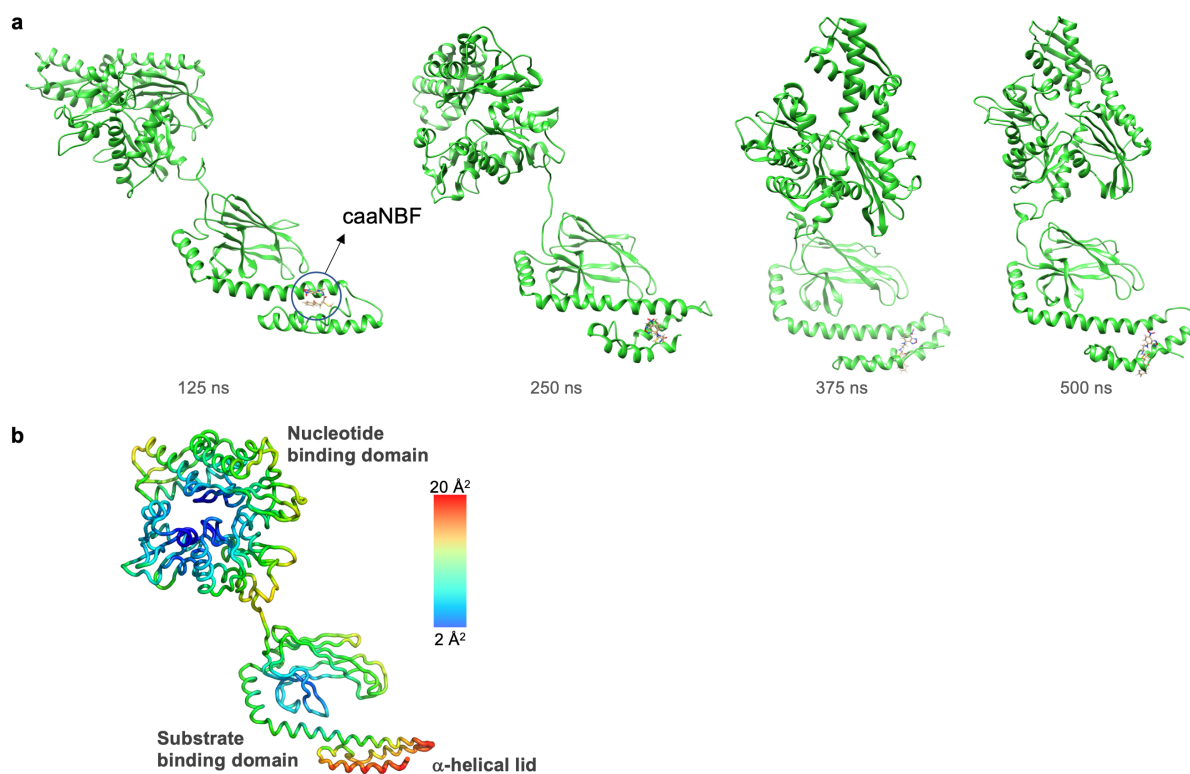


**Figure S5.** Molecular dynamics (MD) simulations on Hsp-caaNBF in explicit water. **a.** Representative frames derived from 0.5  $\mu$ s MD simulation performed on the Hsp-caaNBF conjugate that features the S configuration at the new stereogenic centre generated upon addition of Cys622 to caa-NBF. The NBF moiety is solvent exposed. **b.** Atomic fluctuation ( $C\alpha$ ) analysis of Hsp-caaNBF (S configuration) derived from 0.5  $\mu$ s MD simulations. The data correspond to the average structure of the protein throughout the simulations.

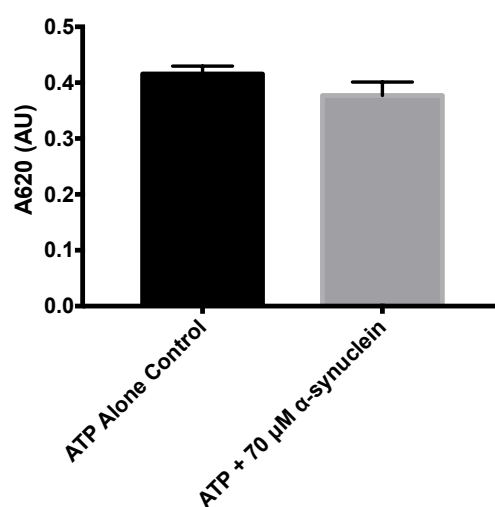


**Figure S6.**  $\alpha$ -synuclein ATPase contamination control. Comparison of A620 values of the background hydrolysis of ATP (black) and in the presence of 70  $\mu$ M  $\alpha$ -synuclein (gray).

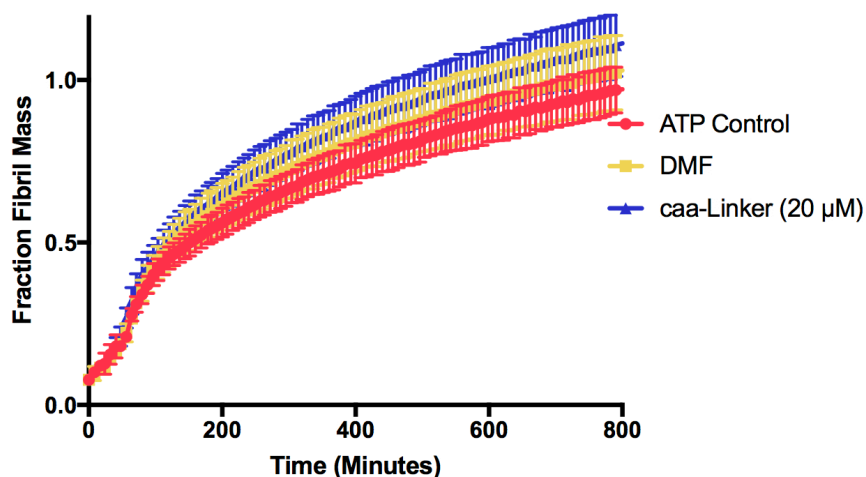


**Figure S7. Control  $\alpha$ -synuclein aggregation assays.** Seeded aggregation of  $\alpha$ -synuclein in the presence of 20  $\mu$ M (in DMF) of the carbonylacrylic linker (caa-Linker, blue), 2  $\mu$ L of dimethylformamide (DMF) (yellow), and the ATP control (red). Neither the linker nor DMF appears to have a detectable effect on the aggregation kinetics.

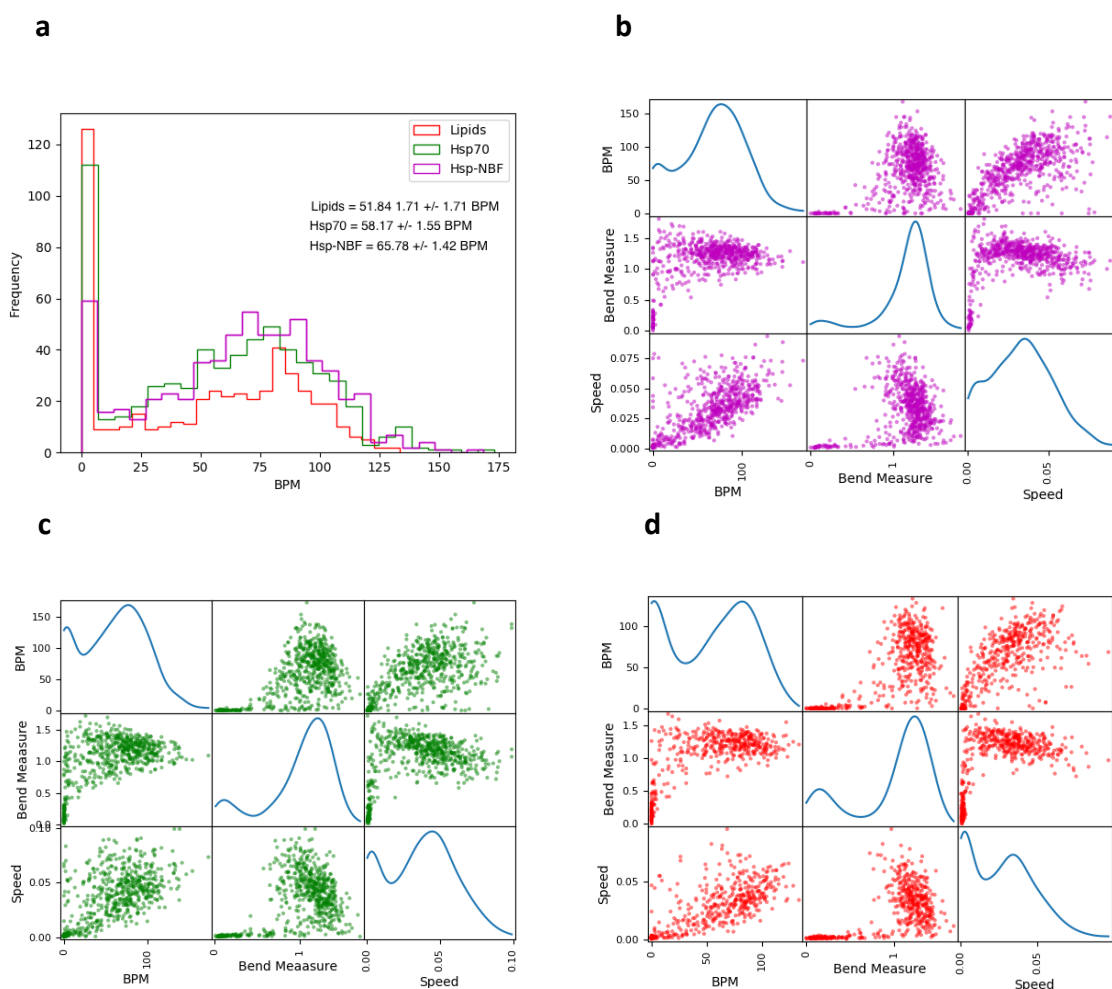


**Figure S8. Comparison of the histograms of combined *C. elegans* treatment populations and scatter matrices.** a. Comparison of the histograms comprising the combined individual



worm BPM measurements from each treatment replicate (bins=25). **b–d**. Population scatter matrices for treated worms plotting the correlation between three different measures: BPM, bend measure, and speed. Diagonals are Kernel Density Estimate plots for the distributions of each individual measurement (B-purple = Hsp-caaNBF, C-green = Hsp70, D-red = lipids).

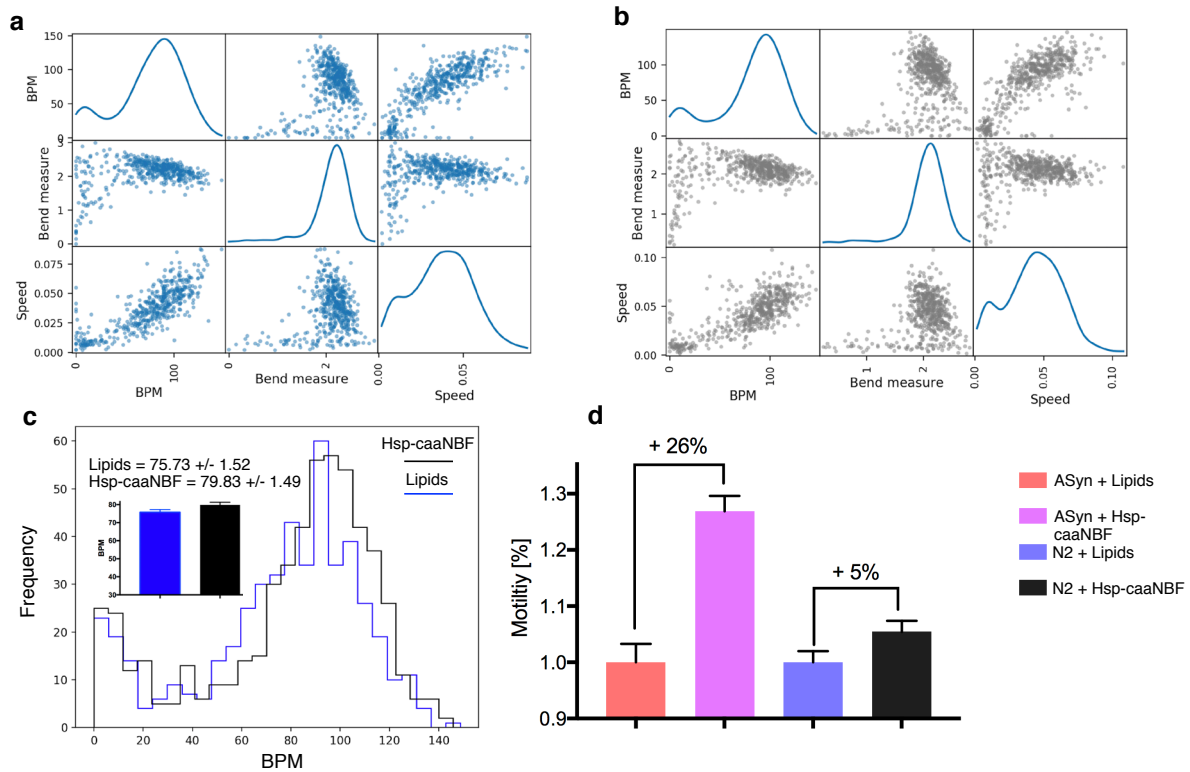


**Figure S9.** Characterizing unspecific benefits of Hsp-caaNBF treatment on wild-type worms. **a,b**. Population scatter matrices of wild-type (N2) worms treated with either empty lipid vesicles (blue) or with Hsp-caaNBF (grey). **c**. Overlaid histograms (bins = 25) of the BPM measurements of the two treatment populations. **d**. Normalized comparisons of the Hsp-caaNBF treatment on ASyn worms versus the N2 worms, displaying that while the modified chaperone has a marginal unspecific benefit in the wild-type worms it is much more beneficial to the worms burdened by protein aggregates.

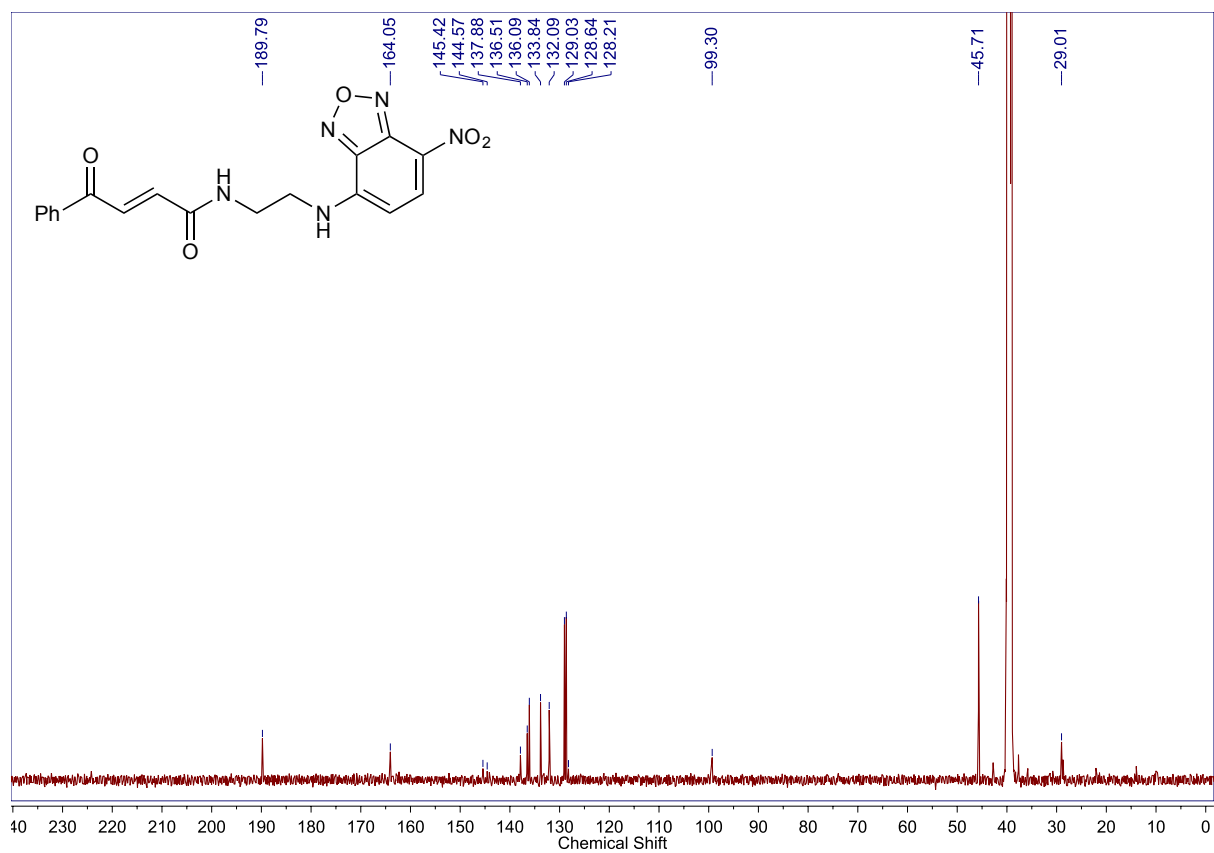
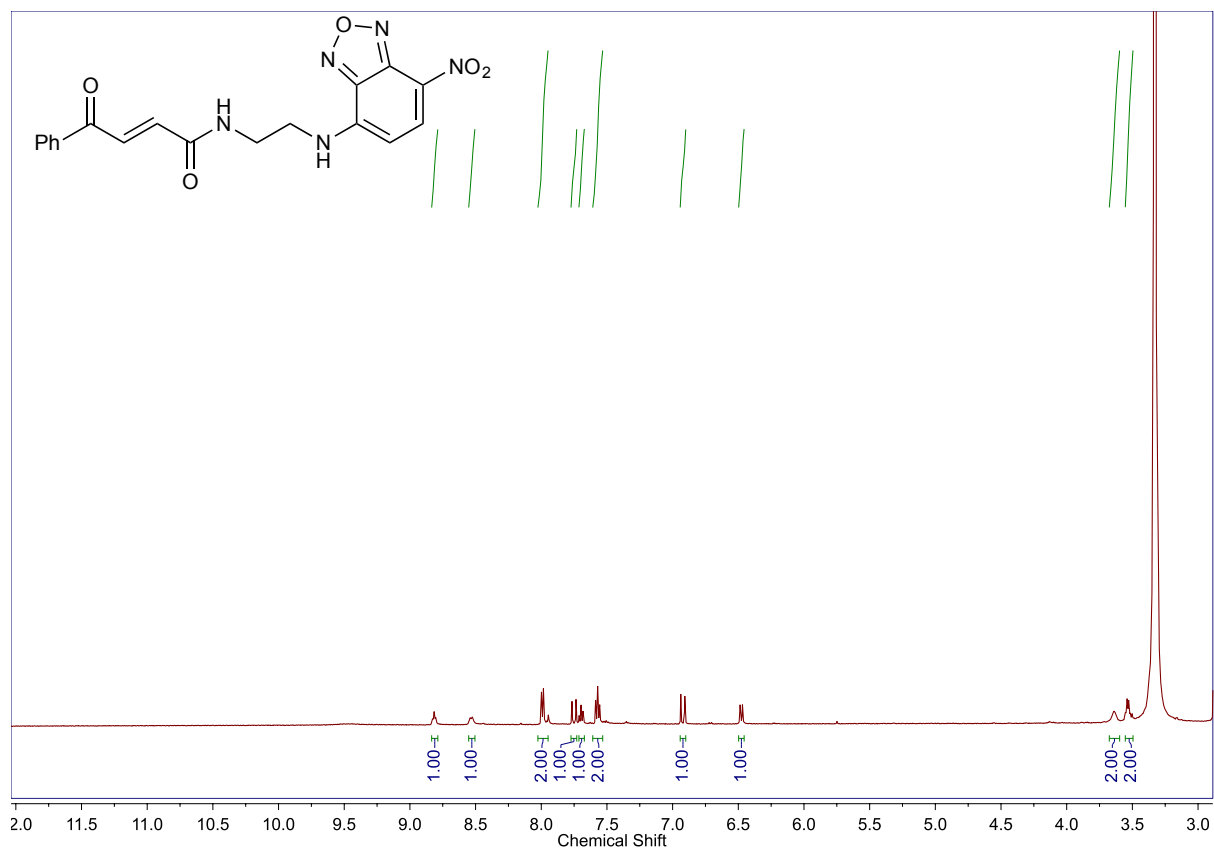


**Figure S10.** <sup>1</sup>H (500 MHz, DMSO-*d*<sub>6</sub>) and <sup>13</sup>C NMR(125 MHz, DMSO-*d*<sub>6</sub>) of caaNBf.

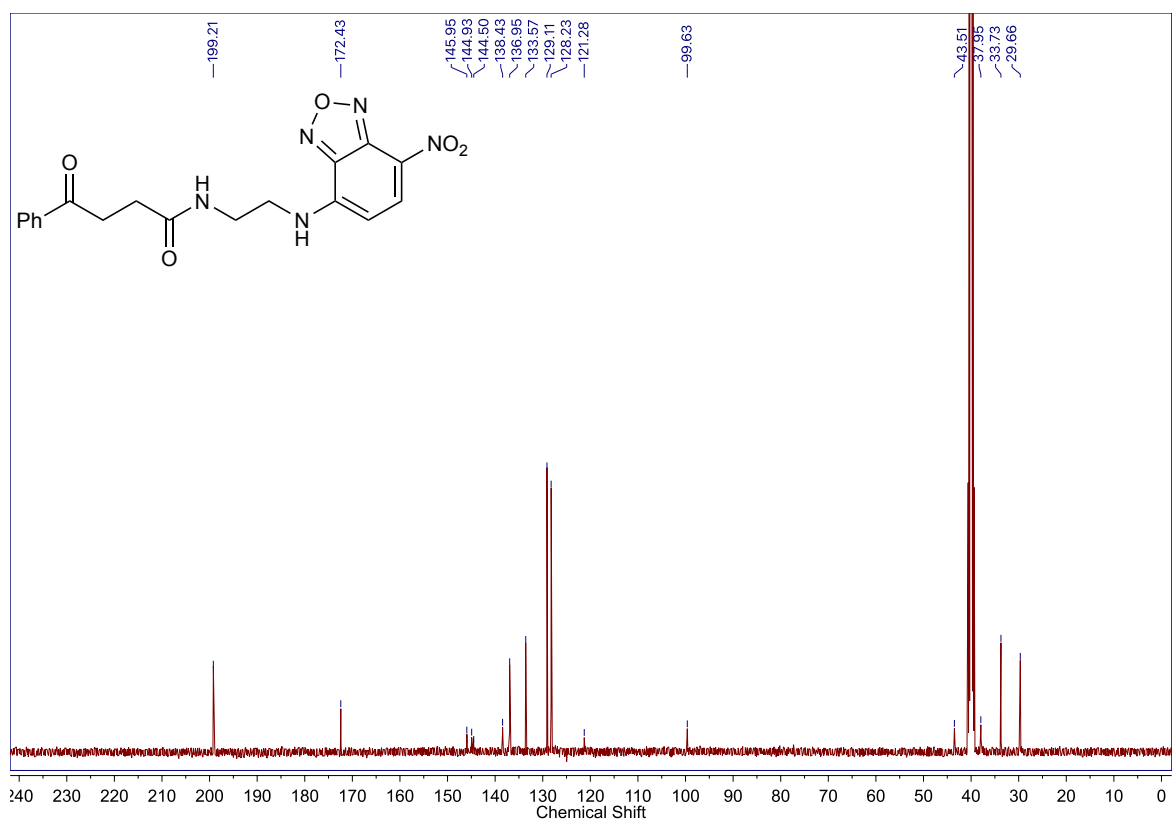
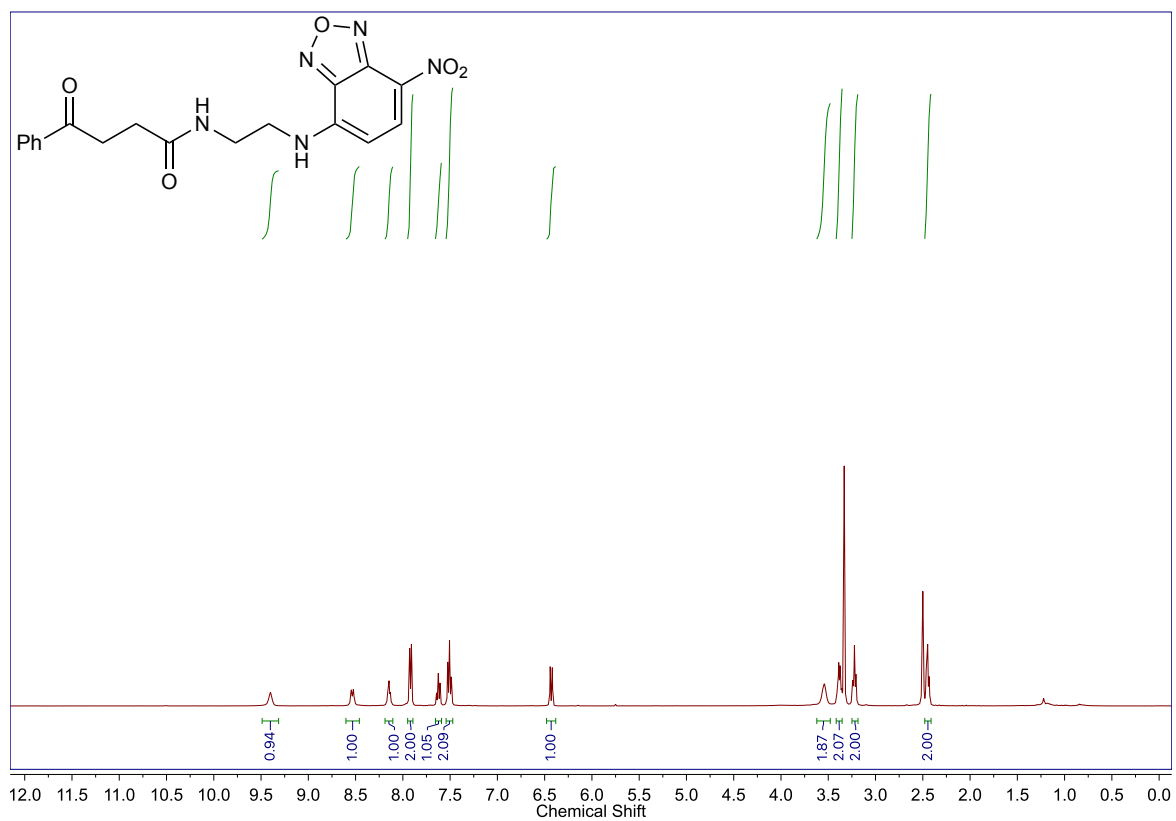


Figure S11. <sup>1</sup>H (400 MHz, DMSO-*d*<sub>6</sub>) and <sup>13</sup>C NMR (100 MHz, DMSO-*d*<sub>6</sub>) of NBF control.

## References

- (1) Aprile, F. A.; Sormanni, P.; Vendruscolo, M. A rational design strategy for the selective activity enhancement of a molecular chaperone toward a target substrate. *Biochemistry* **2015**, *54* (32), 5103–5112.
- (2) Biasini, M.; Bienert, S.; Waterhouse, A.; Arnold, K.; Studer, G.; Schmidt, T.; Kiefer, F.; Cassarino, T. G.; Bertoni, M.; Bordoli, L.; Schwede, T. Swiss-model: Modelling protein tertiary and quaternary structure using evolutionary information. *Nucleic Acids Res.* **2014**, *42*, W252–W258.
- (3) Case, D. A.; Ben-Shalom, I. Y.; Brozell, S. R.; Cerutti, D. S.; Cheatham, III, T. E.; Cruzeiro, V. W. D.; Darden, T. A.; Duke, R. E.; Ghoreishi, D.; Gilson, M. K.; et al. Amber 2018, **2018**, University of California, San Francisco.
- (4) Maier, J. A.; Martinez, C.; Kasavajhala, K.; Wickstrom, L.; Hauser, K. E.; Simmerling, C. Ff14sb: Improving the accuracy of protein side chain and backbone parameters from ff99sb. *J. Chem. Theory Comput.* **2015**, *11* (8), 3696–3713.
- (5) Wang, J.; Wolf, R. M.; Caldwell, J. W.; Kollman, P. A.; Case, D. A. Development and testing of a general amber force field. *J. Comput. Chem.* **2004**, *25* (9), 1157–1174.
- (6) Bayly, C. I.; Cieplak, P.; Cornell, W.; Kollman, P. A. A well-behaved electrostatic potential based method using charge restraints for deriving atomic charges: The RESP model. *J. Phys. Chem.* **1993**, *97* (40), 10269–10280.
- (7) Frisch, M. J.; Trucks, G. W.; Schlegel, H. B.; Scuseria, G. E.; Robb, M. A.; Cheeseman, J. R.; Scalmani, G.; Barone, V.; Petersson, G. A.; Nakatsuji, H.; et al. *Gaussian 16 rev. B.01*, **2016**, Wallingford, CT.
- (8) Jorgensen, W. L.; Chandrasekhar, J.; Madura, J. D.; Impey, R. W.; Klein, M. L. Comparison of simple potential functions for simulating liquid water. *J. Chem. Phys.* **1983**, *79* (2), 926–935.
- (9) Andersen, H. C. Molecular dynamics simulations at constant pressure and/or temperature. *J. Chem. Phys.* **1980**, *72* (4), 2384–2393.
- (10) Miyamoto, S.; Kollman, P. A. Settle: An analytical version of the SHAKE and RATTLE algorithm for rigid water models. *J. Comput. Chem.* **1992**, *13* (8), 952–962.
- (11) Darden, T.; York, D.; Pedersen, L. Particle mesh Ewald: An  $N \cdot \log(N)$  method for Ewald sums in large systems. *J. Chem. Phys.* **1993**, *98* (12), 10089–10092.
- (12) Dolinsky, T. J.; Nielsen, J. E.; McCammon, J. A.; Baker, N. A. PDB2PQR: An automated pipeline for the setup of Poisson-Boltzmann electrostatics calculations. *Nucleic Acids Res.* **2004**, *32*, W665–W667.
- (13) Chang, L.; Bertelsen, E. B.; Wisén, S.; Larsen, E. M.; Zuiderweg, E. R. P.; Gestwicki, J. E. High-throughput screen for small molecules that modulate the atpase activity of the molecular chaperone dnak. *Anal. Biochem.* **2008**, *372* (2), 167–176.

- (14) Brenner, S. The genetics of *Caenorhabditis elegans*. *Genetics* **1974**, *77* (1), 71–94.
- (15) Perni, M.; Aprile, F. A.; Casford, S.; Mannini, B.; Sormanni, P.; Dobson, C. M.; Vendruscolo, M. Delivery of native proteins into *C. elegans* using a transduction protocol based on lipid vesicles. *Sci. Rep.* **2017**, *7* (1), 15045.
- (16) Perni, M.; Galvagnion, C.; Maltsev, A.; Meisl, G.; Müller, M. B. D.; Challa, P. K.; Kirkegaard, J. B.; Flagmeier, P.; Cohen, S. I. A.; Cascella, R.; et al. A natural product inhibits the initiation of  $\alpha$ -synuclein aggregation and suppresses its toxicity. *Proc. Natl. Acad. Sci. U. S. A.* **2017**, *114* (6), E1009–E1017.
- (17) Aprile, F. A.; Sormanni, P.; Perni, M.; Arosio, P.; Linse, S.; Knowles, T. P. J.; Dobson, C. M.; Vendruscolo, M. Selective targeting of primary and secondary nucleation pathways in  $\text{A}\beta_{42}$  aggregation using a rational antibody scanning method. *Sci. Adv.* **2017**, *3* (6), e1700488.
- (18) Bernardim, B.; Cal, P. M. S. D.; Matos, M. J.; Oliveira, B. L.; Martínez-Sáez, N.; Albuquerque, I. S.; Perkins, E.; Corzana, F.; Burtoloso, A. C. B.; Jiménez-Osés, G.; Bernardes, G. J. L. Stoichiometric and irreversible cysteine-selective protein modification using carbonylacrylic reagents. *Nat. Commun.* **2016**, *7*, 13128.